International Journal of Scientific Research & Engineering Trends
Volume 6, Issue 2, Mar-Apr-2020, ISSN (Online): 2395-566X

Convective Heat Transfer & Effect of Temperature Gradient in Super Fluid Helium II

Research Scholar P.V.N. Saichandu, Registrar, Professor, Dr. G. R. Selokar , (Supervision)
Department of Mechanical Engineering,
Sri Satya Sai University of Technology & Medical Sciences Sehore,
Bhopal, M.P, India,
Mail Id:- cponnekanti@gmail.com, selokar1960dr@gmail.com

Abstract - **With a reverberation technique, the speed of the temperature waves (second sound) in fluid helium II has been resolved as an element of temperature from about 1.4°K to the λ-point. The speed is observed to be zero at the λ-point, achieves a limit of 20.46 m/sec. at 1.7°K and diminishes to 19.80 m/sec. at 1.42°K. The precision of the estimations is at any rate ±0.5 percent. The outcomes are in great concurrence with the theoretical expectations of both Tisza and Landau yet will in general support the previous' hypothesis over the latter's. The way that subsequent sound produced in the superfluid can enlist on a mouthpiece stomach drenched in the fluid is examined.**

Heartbeat strategies are connected to the instance of second sound in fluid helium II. Both transmitter and recipient comprise of thermal components and d-c heartbeats are utilized all through. The upsides of beating are counted for the specific instance of second sound. The undifferentiated from electrical circuit is planned for the geometry included. Information is recorded photographically and models for a few cases displayed. Speed of second sound is given as a component of temperature; both the high-temperature and low-temperature reaches are stretched out past those of past examiners utilizing standing wave strategies. Lessening of these d-c heartbeats is given as an element of temperature. The "sifting in time" innate to the beat strategy allows the examination of a few types of coupling between second sound and standard sound.

Keywords- **superfluid helium, Blend, Landau-Khalatnikov etc.**

I. INTRODUCTION

Heat transfer is characterized as vitality in-travel because of temperature contrast. Heat move happens at whatever point there is a temperature angle inside a framework or at whatever point two systems at various temperatures are brought into thermal contact. Heat, which is vitality in-travel, can't be estimated or watched straightforwardly, however the impacts created by it tends to be watched and estimated. Since heat move includes move as well as change of vitality, all heat move procedures must comply with the first and second laws of thermodynamics.

Table -I: Non-Newtonian fluids.

Type of behaviour	Description	Example
Thixotropic	viscosity decreases with stress over time	Honey — keep stirring, and solid hone becomes liquid
Rheopectic	Viscosity increases with stress over time	Cream— the longer you whip it the thicker it gets
Shear thinning	viscosity decreases with increased stress	Tomato sauce
Dilatant or shear thickening	viscosity increases with increased stress	Oobleck

II. LITERATURE REVIEW

explored the heat transfer execution of open thermosyphon with deionized and water based CuO nanofluids as working fluids.

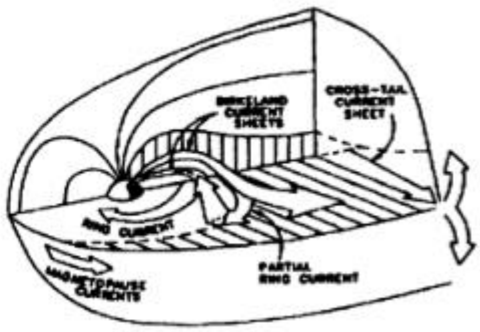

Fig.1.Different current Earth's magnetosphere.

The impact of filling proportion, groupings of nanofluid and working temperatures were examined and it is obvious that for ideal filling proportion of 60% the heat transfer execution of the thermosyphon increments as the power info increments and proposed a push to improve the thermodynamic properties of cryogenic charges, for example, Liquid Oxygen and Liquid Hydrogen, an assortment of systems for delivering sub-cooled or densified cryogenic forces have been investigated and tried. Studies directed by NASA and Boeing have recognized fuel densification as one of the empowering advances for reasonable, solid and safe access to space.

Name	Wave length Range in Microns
Cosmic rays	up to (10^{-6})
Gamma rays	$1(10^{-6})$ to (140×10^{-6})
X-rays	$6(10^{-6})$ to $100,000(10^{-6})$
Ultraviolet rays	0.014 to 0.4
Visible or light rays	0.4 to 0.8
Infrared rays	0.8 to 400
Radio	$10(10^{6})$ to $30,000(10^{6})$

1 micron = 10^{-6} meters

Table –II: Characteristic wave lengths of Radiation.

III. RESEARCH METHODOLOGY

1. Convective Heat Transfer & Effect of Temperature Gradient in Super Fluid (Helium II)

A theoretical verification that Bose buildup occurs in a fluid, for example, superfluid helium was given by Onsager and Penrose. Feynman composed various significant papers during the 1950s, investigating how the properties of fluid helium were firmly identified with the way that the iotas obey Bose insights. The quantization of superfluid flow and the presence of free quantized vortices were proposed hypothetically and autonomously by Onsager and Feynman, and the principal exploratory affirmation originated from crafted by Hall and Vinen with the disclosure of common grating in turning helium and with the immediate perception in a plainly visible examination of the quantization of course. This work prompted thankfulness just because of the full noteworthiness of London's "quantum component on a macroscopic scale", and of the basic significance of Bose buildup in superfluidity.

2. Second Sound

The first observation of this phenomenon was made. Similar experiments were made. The measurement of gives directly the values p and p. The temperature wave present in n s materials other than He-II do not give rise to standing waves as observed in He-II because of energy dissipation and is not observed. Several other experiments on second sound have been reported thereafter.

- **Calculation of Second Sound**

It follows from Jain's theory that the system below Tλ develops a kind of collective binding that could be defined by an energy gap Eg (T) between the normal and superfluid states of the g system. We have

$$E_g(T) = \frac{h^2}{4md_\lambda^3}(d_T - d_\lambda)$$

Once again as suggested by Jain Eg (T) can be used to obtain g the superfluid density p through

$$\rho_s(T) = \frac{E_g(T)}{E_g(0)}\rho$$

and ρn through ρn = ρ – ρs We used the values of Eg (T) obtained by Jain to determine ρs and ρn tabulated ~longwith their values determined by Wood and Hollis Halett [40) from the temperature variation of experimental values of c 2 . We find that the two results agree closely.

The following relation for c2 as a function of temperature was obtained by Peshkov

$$c_2 = \sqrt{\frac{TS^2\rho_s}{C\rho_n}}$$

3. The Phase Diagram of 4He

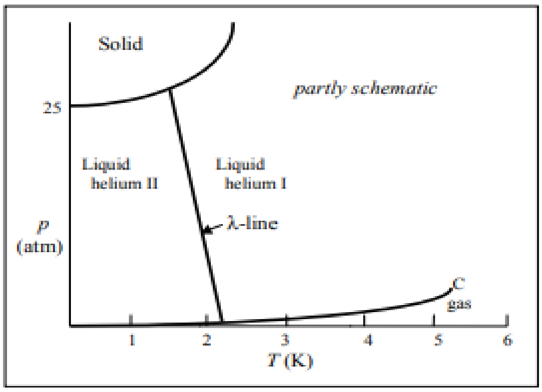

Fig.3.1. The phase diagram of 4He.

The existence of a liquid over a range of pressures at T = 0 must be a quantum effect. It arises from quantum mechanical zero point energy: the fact that a confined particle must have kinetic energy, this energy increasing as the particle is more strongly confined. In the absence of a high pressure, the atoms cannot become sufficiently closely spaced to allow the formation of an ordered crystal, without the penalty of too large a zero point energy.

4. The Heat Capacity

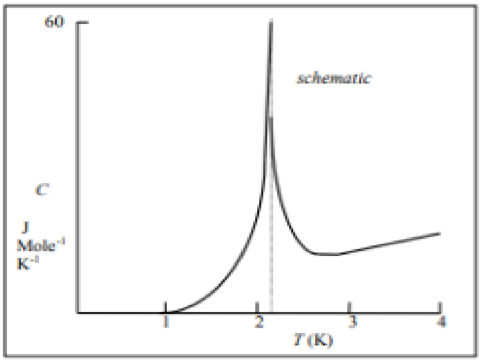

Fig.3.2. The heat capacity of liquid 4He.

The observed Properties of Superfluid 4 He: the Two-Fluid Model

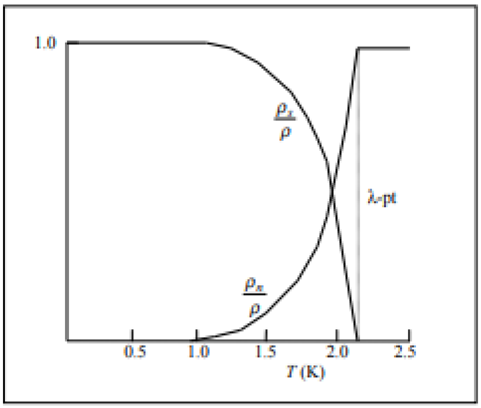

Fig. 3.3. The observed dependence of ρn and ρs on temperature.

3.4 Examples of "Two-Fluid" Behaviour

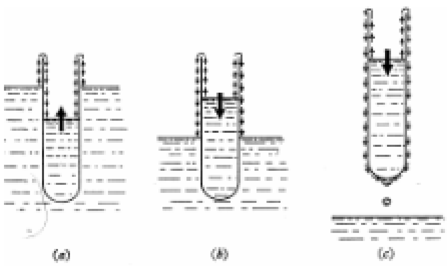

Fig. 3.4. Film flow

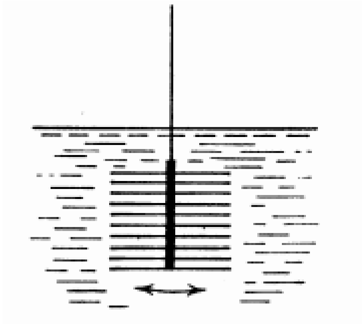

Fig.3.5. The Andronikashvili experiment

3.6 Quantum Restrictions on Superfluid Flow

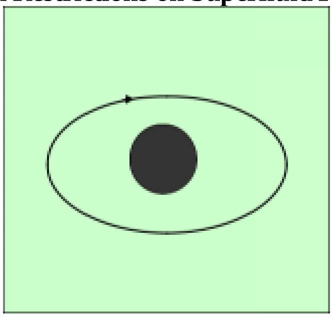

Fig. 3.6. Illustrating a circuit round which there can be a finite superfluid circulation.

If we substitute from equation we obtain,

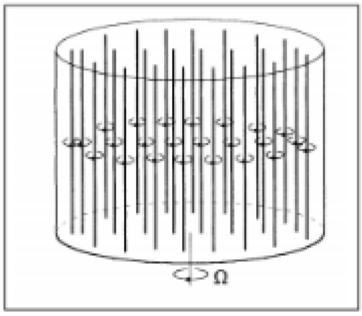

Fig. 3.7. Vortex lines in the uniformly rotating superfluid component.

IV. EXPERIMENT PROCEDURE

1. Thermal Excitation Spectrum of Helium-II

This has in like manner been concentrated to choose the weight dependence of Interatomic power steady. p and 0 have been gotten at different T s ' n from the imperativeness gap and these have been used to find the T dependence of the speed of second sound film thickness and the s speed of third sound has been concentrated to show that the essentialness gap vanishes at the farthest point. The T dependence of the speed of the fourth sound is also gotten. The three points of explicit significance are recognized by their energy (E (q)) and wave vector (q) arranges as on the low energy branch of the basic excitations). They are individually known as roton,

International Journal of Scientific Research & Engineering Trends
Volume 6, Issue 2, Mar-Apr-2020, ISSN (Online): 2395-566X

maxon, and level modes. They assume a significant job in choosing different properties of He-II.

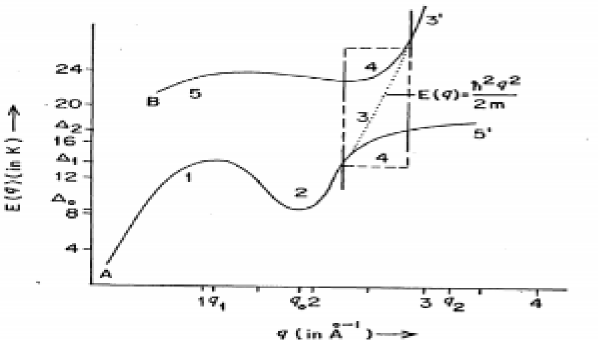

Fig.4.1. The Typical nature of the Thermal Excitation Spectrum as .observed experimentally by the neutron inelastic scattering.

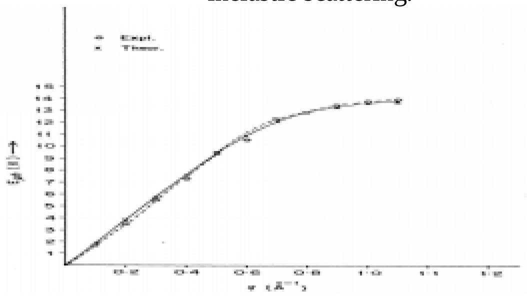

2. Comparison of Energy Eph obtained that observed experimentally

Table -III: Experimental and theoretical values of Vp , Vg and Eph for different values of q

q	expt.	theor.	expt.	theor.	expt.	theor.
	V_p^*	V_p	V_g^{**}	V_g	E_{ph}^{***}	E_{ph}
A^{o-1}	m/sec	m/sec	m/sec	m/sec	K	K
	1	2	3	4	5	6
0.0	237.7	238.0	237.7	238.3	00.00	00.00
0.1	241.3	243.7	238.5	248.4	01.69	01.86
0.2	245.3	246.9	240.5	251.4	03.48	03.78
0.3	248.7	247.9	242.5	248.2	05.54	05.69
0.4	247.3	247.0	240.5	239.9	07.27	07.55
0.5	242.6	244.9		189.4	09.54	10.15
0.6	233.9	236.7		161.0	10.60	10.86
0.7	221.3	224.4		128.8	12.31	12.01
0.8	206.6	209.4		095.7	12.87	12.81
0.9		193.8		063.9	13.69	13.34
1.0		179.1		031.5	13.79	13.69
1.1		164.6		000.8	14.46	13.84

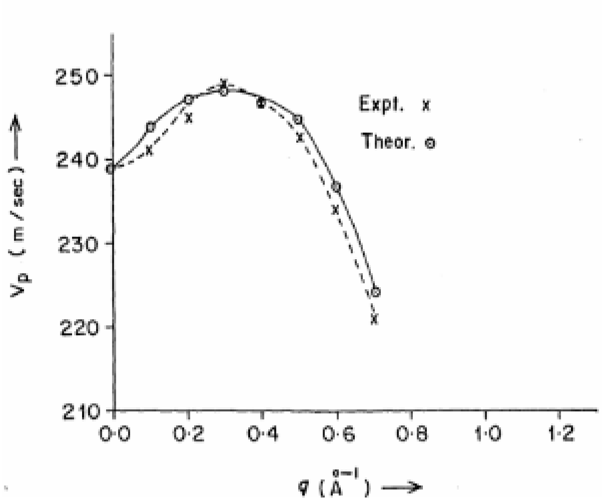

Fig.4.3. Comparison of phase velocity v obtained theoretically p with that observed experimentally.

Table -IV: Accidental degeneracy of the single particle excitation and the multi-phobon mode at about

				theor.		expt.	
q	E_1	E_2	ϵ	E^+	E^-	E^{+*}	E^{-*}
A^{o-1}	K	K	K	K	K	K	K
2	22	09.34	4.5	23.43	7.90	23.7	9.3
2.1	22	09.88	4.5	23.49	8.40	22.8	10.3
2.2	22	11.56	4.5	23.67	9.89	23.7	11.7
2.3	22	14.34	4.5	24.07	12.26	24.7	13.4
2.4	22	18.22	4.5	24.99	15.23	26.6	16.1
2.5	22	23.23	4.5	27.15	18.07	29.9	19.0
2.6	22	29.34	4.5	31.48	19.86	35.1	19.9
2.7	22	36.56	4.5	37.84	20.72	41.8	20.5

Fig.4.4. Comparison of theoretically and experimentally (dotted line) observed curve of mixing of the single particle excitation and the multi-phonon mode.

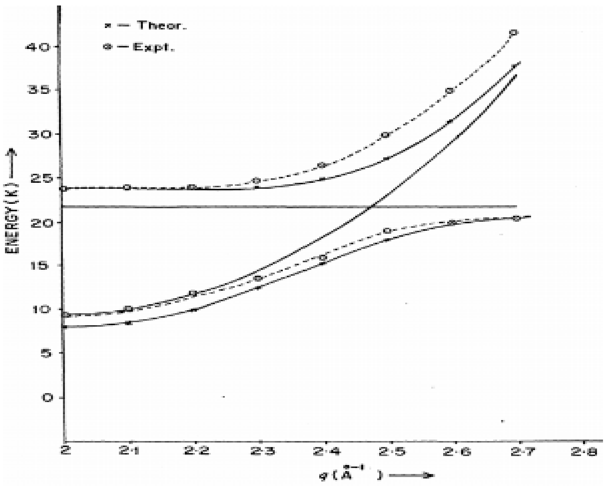

International Journal of Scientific Research & Engineering Trends
Volume 6, Issue 2, Mar-Apr-2020, ISSN (Online): 2395-566X

V. HEAT TRANSFER & EFFECT OF TEMPERATURE GRADIENT IN SUPER FLUID

At temperatures underneath Tλ ≈ 2.18 K liquid helium experiences a stage progress, from an old style fluid (He I) to quantum one (He II). The last stage shows numerous particular properties among which the capacity to flow without evident dispersal through dainty vessels, the quantization of the speed in nuclear breadth vortex fibers, and an effective heat transport related with the presence of temperature waves ("second sound")1 . Those properties are surely known in the system of the two-fluid model: He II is depicted as a blend of a "typical fluid" and a "superfluid". The first is viscous and conveys all the entropy of the fluid, while the second is inviscid and irrigational aside from on the quantum vortices. The present work was roused by the exploratory study of disturbance in He II, and related speed sensors. In traditional fluids, a typical picture of violent motion is the Richardson course: the biggest vortexes of the flow are consistently extended creating littler and littler whirlpools with no huge energy misfortune in the "course" process. This procedure holds until whirlpools are little enough for the viscous scattering to wind up huge. A decent representation of this procedure is given by the appropriation of the motor energy as an element of the flow scale.

5.1 Velocity Equations and Momentum Conservation

$$\frac{\rho_n}{\rho}\nabla p + \rho_s s\nabla T + \rho\frac{\partial \mathbf{v}}{\partial t} - \rho_s\frac{\partial \mathbf{v}_s}{\partial t} + A\rho_s\rho w^2(\mathbf{v}-\mathbf{v}_s) = \rho_n\mathbf{g}$$

$$\frac{1}{\rho}\nabla p - s\nabla T + \frac{\partial \mathbf{v}_s}{\partial t} - A\rho w^2(\mathbf{v}-\mathbf{v}_s) = \mathbf{g}$$

5.2 Temperature Equation and Energy Conservation

$$\rho C_v\frac{\partial T}{\partial t} + \rho\beta C_v T\nabla\cdot\mathbf{v} + \rho C_v\mathbf{v}\cdot\nabla T + T\frac{\rho\rho_s}{\rho_n}s\nabla\cdot\mathbf{v} - T\frac{\rho\rho_s}{\rho_n}s\nabla\cdot\mathbf{v}_s - \nabla\cdot(k\nabla T) = q$$

5.3 Convergence Error

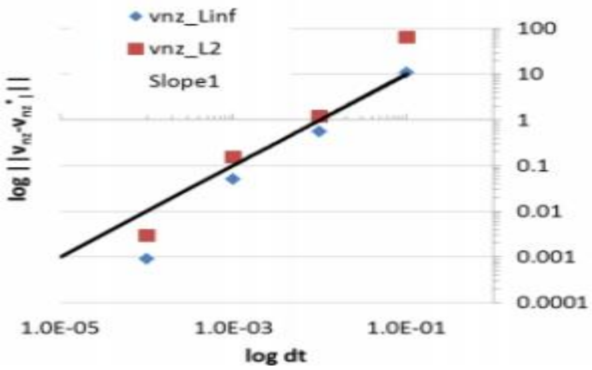

Fig. 5.1. Convergence in time for the EB scheme

VI. RESULTS AND DISCUSSIONS

In this section, we exhibit the utilization of the new solver and the adaptability of the new code by unraveling the protection adjusts of superfluid helium in pertinent geometries up to the third measurement. The present outcomes utilize an essential registering limit, for example double center, Intel® processor, 2.2 GHz, 4 GB of introduced memory (RAM). Note that the models picked don't deplete the code abilities. For instance, constrained flow conduct in He II can likewise be portrayed by this solver, just as recreation including temperature, heat motion or weight as boundary conditions. We found that the soundness of the arrangement frequently relies upon the decision of a physically predictable arrangement of boundary conditions.

6.1 Test Case1: Second sound propagation in 1-D

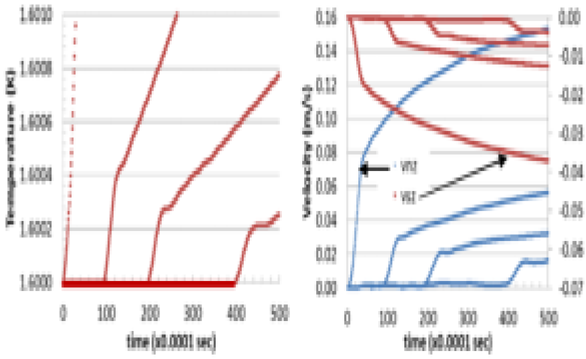

Fig.6.1. Propagation of the temperature and velocities waves at 1.62 K. c2=21.97 m/s

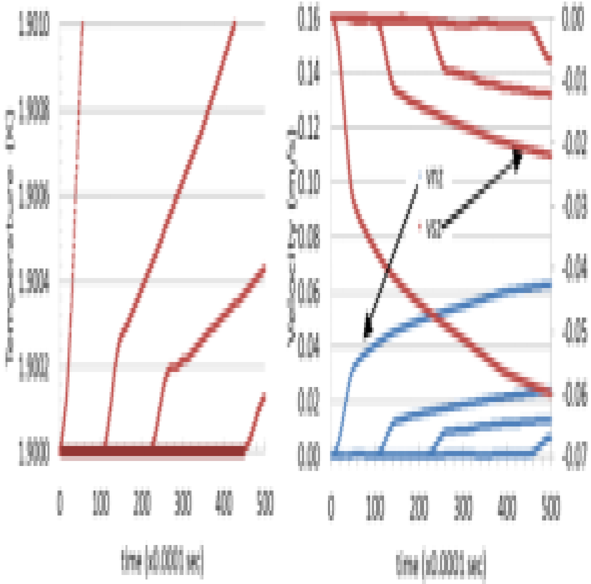

Fig. 6.2. Propagation of the temperature and velocities waves at 1.9 K. c2=19.96

International Journal of Scientific Research & Engineering Trends
Volume 6, Issue 2, Mar-Apr-2020, ISSN (Online): 2395-566X

6.2 Test Case3: Internal convection in 2 and 3-D Models

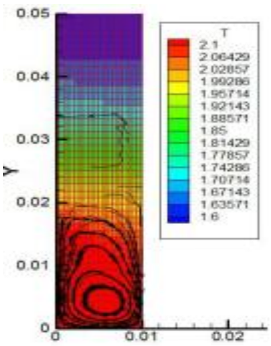

Fig.6.1(a). Superfluid component velocity when a constant heat flux is applied on half of the bottom left side. Mesh composed of 640 quadrilaterals FE (Temp. Bath = 1.8 K).

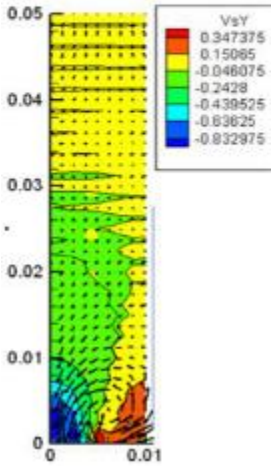

Fig.6.2(b). Superfluid component velocity streamline when a constant heat flux is applied on half of the bottom left side. Mesh composed of 1,728 quadrilaterals FE (Temp. Bath = 1.6 K)

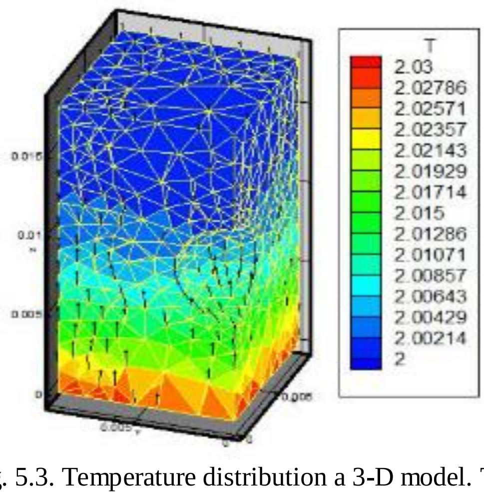

Fig. 5.3. Temperature distribution a 3-D model. The arrows represent the normal component velocities

VII. CONCLUSION

We have investigated the stage graph of fluid helium blends. While traditional hypothesis neglects to give an unmistakable image of the stage detachment, Jain's hypothesis gives a tasteful clarification by expecting His pair arrangement. Further, our gauge of the underlying incline of the A line concurs intimately with the trial esteem. Utilizing the articulations for substance potential given by Macro-orbital hypothesis, we have evaluated the decrease of the A point in the blend as a component of 3He fixation. Our outcome intently concurs with exploratory qualities.

Helium has two stable isotopes: 4He and 3He. While 4 He is a boson with atomic turn I= 0, 3He is a fermion with atomic turn I= 1/2. Both the isotopes have exceptionally frail Vander Waals holding and enormous zero point energies. The interchange of the frail restricting power and the enormous zero point vitality makes the two isotopes stay fluid under soaked vapor weight notwithstanding for T - + 0. Moreover, this is likewise in charge of the way that the two isotopes have the most reduced bubbling temperatures and basic focuses known for any substance in nature.

REFERENCES

[1]. Ramana Rcddy J.V., Sugunanlnla V., Sandccp N., Thcrnio diffusion and hall current effects on an unstcady flow of a nanofluid undcr thc influcncc of inclined magnetic field. Int. J. Eng. Res. Afr. 20 (2015) 61-79.

[2]. Sulochana C., Sandeep N, Sugunarnma V., Rushi kumar B., Aligned magnetic field and cross diffusion effects of a nanofluid over an exponentially stretching surface in porous medium. Appl. Nanosci. (201 5) 1-10, DOI: 10.1007/sI 3204- 01 5-0475-X.

[3]. Sandeep N., Sugunamma V., Mohankrishna P., Effects of radiation on an unsteady natural convectivc flow of a EG-Nimonic 80a nanofluid past an infinite vertical plate. Adv. Phy. Theories Appl. 23 (2014) 36-43.

[4]. Rashidi M.M., Pour S.A.M., llayat T, Obaiditt S, Analytic approxinrate solutions for steady flow over a rotating disk in porous medium with heat transfer by homotopy analysis method. Comp. Fluids 54 (201 2) 1-9.